Facial Dysmorphism Across the Fetal Alcohol Spectrum

AUTHORS: Michael Suttie, MSc,[a] Tatiana Foroud, PhD,[b] Leah Wetherill, MSc,[b] Joseph L. Jacobson, PhD,[c,d,e] Christopher D. Molteno, MD,[e] Ernesta M. Meintjes, MD,[d] H. Eugene Hoyme, MD,[f] Nathaniel Khaole, MD,[d] Luther K. Robinson, MD,[g] Edward P. Riley, PhD,[h] Sandra W. Jacobson, PhD,[c,d,e] and Peter Hammond, PhD[a]

[a]Molecular Medicine Unit, UCL Institute of Child Health, London, United Kingdom; [b]Department of Medical and Molecular Genetics, Indiana University School of Medicine, Indianapolis, Indiana; [c]Department of Psychiatry and Behavioral Neurosciences, Wayne State University School of Medicine, Detroit, Michigan; Departments of [d]Human Biology and [e]Psychiatry and Mental Health, University of Cape Town, Faculty of Health Sciences, Cape Town, South Africa; [f]Sanford School of Medicine, University of South Dakota, Vermillion, South Dakota; [g]State University of New York, Buffalo, New York; and [h]Department of Psychology, College of Sciences, San Diego State University, San Diego, California

KEY WORDS

facial dysmorphism, fetal alcohol spectrum disorders, fetal alcohol syndrome, dense surface modeling, signature graphs, prenatal alcohol exposure, alcohol-related neurodevelopmental disorder

ABBREVIATIONS

CVLT-C—California Verbal Learning Test—Children's Version
3D—3-dimensional
DSM—dense surface model
FAS—fetal alcohol syndrome
FASD—fetal alcohol spectrum disorder
HC—healthy control
HE—nonsyndromal heavy alcohol exposure
HE1—nonsyndromal heavy exposed with FAS/PFAS-like face signature
HE2—nonsyndromal heavy exposed with more control-like face signature
PFAS—partial fetal alcohol syndrome
ROC—receiver operating characteristic
UCT—University of Cape Town
WISC IV—Fourth edition of Wechsler Intelligence Scale for Children

Dr Foroud, Ms Wetherill, and Drs J. Jacobson, Molteno, and S. Jacobson were responsible for acquisition of data. Assessment of participants was conducted by Drs Molteno, Meintjes, J. Jacobson, S. Jacobson, Hoyme, Khaole, and Robinson. Mr Suttie, Dr Foroud, Ms Wetherill, and Drs J Jacobson, S. Jacobson, and Hammond analyzed the data. Design and management of study were conducted by Drs Foroud, Riley, S. Jacobson, and Hammond, and Mr Suttie, Dr Foroud, Ms Wetherill, and Drs Riley, S. Jacobson, and Hammond wrote the article.

(Continued on last page)

WHAT IS KNOWN ON THIS SUBJECT: Prenatal alcohol exposure causes a continuum of effects. The most severe phenotype, fetal alcohol syndrome, involves facial dysmorphism, growth deficits, and neurocognitive problems. The classic facial characteristics include short palpebral fissures, smooth philtrum, and thin upper vermillion.

WHAT THIS STUDY ADDS: This study develops novel strategies to help detect facial dysmorphism across the fetal alcohol spectrum, especially in children with heavy alcohol exposure but without classic facial characteristics. The methods show potential for identifying which of these children are cognitively affected.

abstract

OBJECTIVE: Classic facial characteristics of fetal alcohol syndrome (FAS) are shortened palpebral fissures, smooth philtrum, and thin upper vermillion. We aim to help pediatricians detect facial dysmorphism across the fetal alcohol spectrum, especially among nonsyndromal heavily exposed (HE) individuals without classic facial characteristics.

METHODS: Of 192 Cape Coloured children recruited, 69 were born to women who reported abstaining from alcohol during pregnancy. According to multifaceted criteria, the remainder were allocated clinically to the FAS (n = 22), partial FAS (n = 26) or nonsyndromal HE (n = 75) categories. We used dense surface modeling and signature analyses of 3-dimensional facial photographs to determine agreement between clinical categorization and classifications induced from face shape alone, to visualize facial differences, and to consider predictive links between face shape and neurobehavior.

RESULTS: Face classification achieved significant agreement with clinical categories for discrimination of nonexposed from FAS alone (face: 0.97–1.00; profile: 0.92) or with the addition of partial FAS (face: 0.90; profile: 0.92). Visualizations of face signatures delineated dysmorphism across the fetal alcohol spectrum and in half of the nonsyndromal HE category face signature graphs detected facial characteristics consistent with prenatal alcohol exposure. This subgroup performed less well on IQ and learning tests than did nonsyndromal subjects without classic facial characteristics.

CONCLUSIONS: Heat maps and morphing visualizations of face signatures may help clinicians detect facial dysmorphism across the fetal alcohol spectrum. Face signature graphs show potential for identifying nonsyndromal heavily exposed children who lack the classic facial phenotype but have cognitive impairment. *Pediatrics* 2013;131:e779–e788

Prenatal alcohol exposure causes a continuum of effects. The most severe phenotype, fetal alcohol syndrome (FAS), affects face shape, growth, and neurobehavior.[1,2] Fetal alcohol spectrum disorders (FASDs) include FAS and other pathologies arising from prenatal alcohol exposure. Table 1 summarizes criteria we used to characterize FAS and partial FAS (PFAS) and to differentiate them from those with nonsyndromal heavy alcohol exposure (HE), where our criteria were not met, and from nonexposed controls (HCs). Classic FAS facial characteristics of short palpebral fissures, smooth philtrum, and thin upper lip vermillion[3] overlap with conditions that pediatricians consider as differential diagnoses[4] (Table 2).

Several studies have explored image-based recognition of FAS facial features.[5–15] Often, the use of linear measures alone limited shape analysis. We used sparse landmarks to induce a correspondence of 25 000+ points on a face enabling dense surface model (DSM) analysis of shape. Previously, such analyses delineated facial features in neurodevelopmental disorders establishing discriminating characteristics and phenotype-genotype correlations,[16–26] including a murine model of ethanol exposure.[27]

In this study of South African children, we used face shape to induce classification schemes and tested agreement with clinical FASD categorization. The more heterogeneous phenotype of HE forced us to introduce a clustering technique,[28] signature graph analysis,[29,30] which normalizes face shape and links individuals with similar facial dysmorphism. Signature graph analysis identified half of our HE group as having facial dysmorphism that was more FAS-like than control-like. These individuals with HE performed less well on psychometric tests than did individuals with HE who facially were more control-like. We also demonstrated that heat map comparisons of, and animated morphs between, individual faces and matched control means represent facial dysmorphism that was otherwise overlooked. We conclude that these visualizations and signature analyses can help pediatricians detect facial dysmorphism across the fetal alcohol spectrum.

METHODS

Participants

The 192 participants were from 2 longitudinal University of Cape Town (UCT) cohorts recruited from the local Cape coloured (mixed ancestry) community,[31,32] where the incidence of heavy alcohol use during pregnancy and FAS are among the highest in the world. In one cohort (N = 137),[31] drinking histories of mothers were obtained prospectively by using a timeline follow-back interview[33] administered at recruitment in antenatal clinics, during pregnancy, and at 6 weeks postpartum, to ascertain third trimester drinking. Heavy drinkers consumed ≥14 standard drinks per week or participated in binges of ≥5 drinks per occasion. Controls reported abstaining from drinking during pregnancy. Alcohol-consuming pregnant women were advised to modify intake and referred for help. In the second cohort (N = 55),[32,34] 24 children were older siblings of children in the first cohort. The remainder, alcohol exposed and controls, were identified by screening children in a school in a rural area with high incidence of alcohol abuse. Ethical approval was obtained at Wayne State University and UCT. Written informed consent was obtained from mothers and oral assent was obtained from children.

Clinical and Neurobehavioral Assessments

We organized a community clinic in which each child was examined for growth deficits and FAS facial features independently by expert dysmorphologists (H.E.H., L.K.R.)[31,32] blinded to prenatal alcohol exposure history, using a standard protocol[2] and the Astley Lip-Philtrum Guide14. There was substantial agreement between them on assessment of dysmorphism, including published philtrum and vermilion rating scales[35] and palpebral fissure length (r = 0.80, 0.84, and 0.77, respectively), and between them and another dysmorphologist (N.K.) who examined a small subset not seen at the clinic (median r = 0.78). Subsequently, there was agreement on the final FASD categorization (H.E.H., L.K.R., S.W.J., C.D.M., J.L.J.). Offspring of abstaining or low-consumption mothers were designated as HCs, unless they met FAS criteria.[2] Three children whose mothers denied drinking during pregnancy met FAS criteria. Individuals with genetic disorders were excluded. As part of the UCT longitudinal FASD studies, neurobehavioral assessment was undertaken at 9-year follow-up[31,32,36] and included fourth edition of Wechsler Intelligence Scale for Children (WISC IV),[37] to measure IQ, verbal comprehension and perceptual reasoning, and California Verbal Learning Test–Children's Version (CVLT-C),[38–40] to measure recall of words learned over consecutive trials and recognition memory after a 20-minute delay. Testing was conducted by Master's level neuropsychologists in the primary language (Afrikaans or English) used in a child's home and school. The neuropsychologists were blinded to prenatal alcohol exposure and FASD categorization, except in severe cases.

Face Analysis

All 3-dimensional (3D) facial images were captured with a commercial photogrammetric camera (3dMD Inc, Atlanta). One author (M.S.) landmarked each image at 24 validated locations[41] (Supplemental Fig 1). A DSM constitutes principal component analysis modes covering 99% of

TABLE 1 Clinical Categorization

	Criteria	FAS	PFAS	HE
Alcohol exposure	Confirmed maternal consumption throughout gestation	—	√	≥1 oz AA/d or ≥4 binges: each ≤2 oz AA
Face	Short palpebral fissure (≤10th percentile) Thin upper lip (4 or 5 on Astley scale) Smooth philtrum (4 or 5 on Astley scale)	≥2 of 3	≥2 of 3	—
Growth	Delay for height or weight (≤10th percentile)	√	√	—
Head/Brain	Reduced circumference (≤10th percentile) CNS structural abnormality	≥1 of 2	≥1 of 3	—
Behavior	Evidence of behavioral or cognitive deficiency	—	≥1 of 3	—

AA, absolute alcohol; 1 oz AA ≈ 2 standard drinks.

shape variation in the faces analyzed.[20,30] Landmarking and DSM building were undertaken using software developed in-house.[20,30] The agreement of clinical categorization (Table 1) and classification using DSM representation of face shape was estimated from 20 random 90% to 10% training-unseen test pairs of subject subsets (stratified with respect to affected or unaffected status) by using receiver operating characteristic (ROC) curve analysis. To analyze the faces of those who were HE, we introduced signature graph[28–30] cluster analysis. Sequences of 35 contiguously aged control faces generated age-matched means for comparison and normalization. A paucity of controls forced gender aggregation when normalizing. Displacement orthogonal to the face surface at 25 000+ points was normalized with respect to displacements at corresponding points on age-matched reference faces to produce a face signature. Analogous processes produced signatures for lateral, vertical, and depth axes. Face signatures were visualized as heat maps to depict normalized contraction, coincidence, and expansion compared with matched controls. For a pair of signatures, face signature distance (FSD) calculated the difference in facial dysmorphism as the square root of summed squared differences across all surface points. Each face signature was linked to another with shortest FSD from it, generating signature clusters themselves linked by closest constituent signatures to form a connected signature graph[30] drawn using GraphViz.[42]

RESULTS

Sample Characteristics

The 96 male and 96 female children had no sex or age distribution differences (Table 3). Drinking levels among HE groups did not differ statistically. Alcohol-consuming mothers reported an average of 2.8 standard drinks per day

TABLE 2 Conditions to Be Considered as a Differential Diagnosis for FASD

Syndrome/Condition	Features Overlapping With FASD	Differentiating Features
Aarskog	Small nose with anteverted nares, broad philtrum, maxillary hypoplasia, and wide-spaced eyes	Rounded face, down-slanted palpebral fissures, widow's peak, crease below lower lip, incomplete out folding of upper helices, and dental eruption problems
Cornelia de Lange	Long philtrum, thin vermillion border, anteverted nares, and depressed nasal bridge	Single, bushy eyebrow extending across forehead, long eyelashes, downturned mouth, high arched palate, and short limbs/stature
Dubowitz	Short palpebral fissures, wide spaced eyes, and epicanthal folds	Shallow supraorbital ridge with nasal bridge near the level of the forehead, and broad nasal tip
Fetal hydantoin (filantin)	Wide-spaced eyes and depressed nasal bridge	Short nose with bowed upper lip
Fetal valproate	Epicanthal folds, anteverted nares, long philtrum with thin vermillion border, and wide-spaced eyes	High forehead, infraorbital crease or groove, and small mouth
Maternal phenylkeonuria fetal effects	Epicanthal folds, short palpebral fissures, long underdeveloped philtrum, and thin vermillion border	Small upturned nose, round facies, and prominent glabella
Noonan	Low nasal bridge, wide-spaced eyes, and epicanthal folds	Down-slanted palpebral fissures, keratoconus, wide mouth, and protruding upper lip
Toluene embryopathy	Short palpebral fissures, mid-face hyoplasia, smooth philtrum, and thin vermillion border	Micrognathia, large anterior fontanel, down-turned mouth corners, hair patterning and ear abnormalities, and bifrontal narrowing
Williams	Short palpebral fissures, anteverted nares, long philtrum, depressed nasal bridge, and epicanthal folds	Wide mouth with full lips, stellate pattern of the iris, periorbital fullness, and connective tissue disorders

Data available at www.cdc.gov/ncbddd/fasd/documents/fas_guidelines_accessible.pdf

TABLE 3 Sample Characteristics (N = 192)

	FAS (n = 22)	PFAS (n = 26)	HE (n = 75)	HC (n = 69)	F or χ^2
Age at 3D photo (years)	10.6 ± 2.4	10.0 ± 1.5	10.4 ± 2.7	10.1 ± 2.6	0.46
Sex n (% male)	12 (54.5%)	14 (53.8%)	36 (48.0%)	34 (49.3%)	0.47
Parity	2.9 ± 1.4	2.8 ± 1.9	1.7 ± 1.0	2.0 ± 1.2	8.27***
Height (cm)	127.0 ± 13.1	131.0 ± 10.4	136.6 ± 13.6	135.6 ± 14.1	3.68*
Wt (kg)	25.8 ± 7.2	27.8 ± 6.4	34.0 ± 10.9	34.2 ± 13.2	5.29**
Head circumference (cm)	49.9 ± 1.4	51.6 ± 1.4	53.0 ± 1.7	53.0 ± 1.9	22.55***
BMI	15.7 ± 1.6	16.0 ± 1.3	17.8 ± 3.2	18.0 ± 3.9	5.05**
Facial anomalies					
Short palpebral fissures	18 (81.8%)	18 (69.2%)	9 (12.0%)	8 (11.6%)	72.89***
Flat philtrum	20 (90.9%)	25 (96.2%)	22 (29.3%)	15 (21.7%)	69.13***
Thin vermillion	20 (90.9%)	25 (96.2%)	20 (26.7%)	17 (24.6%)	68.34***
Child's WISC IV-IQ	60.6 ± 11.1	65.3 ± 10.4	71.1 ± 12.8	75.3 ± 12.0	7.82***
Alcohol use during pregnancy					
oz AA/day	1.8 ± 2.4	1.2 ± 1.2	1.3 ± 1.8	0.0 ± 0.0	14.65***
oz AA/occasion	4.7 ± 2.8	4.2 ± 2.8	4.4 ± 4.0	0.0 ± 0.0	35.33***
Frequency (days/week)	2.0 ± 1.9	1.9 ± 1.0	1.7 ± 1.4	0.0 ± 0.0	36.65***
Cigarettes/day during pregnancy	6.3 ± 6.2	7.4 ± 5.3	8.0 ± 7.1	4.3 ± 7.4	3.68*

Values are mean ± SD or %. AA, absolute alcohol; 1 oz AA ≈ 2 standard drinks. Cut-points for facial anomalies: short palpebral fissures, ≤10th percentile; flat philtrum and thin vermillion, rank 4 or 5 on Astley Lip-Philtrum Guide 1. The palpebral fissure measurements were obtained by using a rigid ruler, marked in millimeters according to standard methods, and were compared with published norms[46]; centiles were recorded. Mothers of PFAS and HE children smoked more than mothers of controls ($P < .05$ and .01, respectively). Mothers of FAS and PFAS children were higher in parity than were mothers of children with HE and controls (all $P < .01$). Maternal age at delivery for FAS children was higher than for mothers of children with HE and HCs ($P < .01$) and PFAS compared with children with HE ($P < .05$). Dose-dependent relations for head circumference: FAS < PFAS < HE and controls ($P < .001$); height and weight: FAS < HE and controls ($P < .01$); weight: PFAS < HE and controls ($P < .01$). WISC IQ: FAS < HE and controls ($P < .002$); PFAS < controls ($P < .002$); PFAS < HE ($P = .055$); HE < controls ($P < .10$); FAS and PFAS < controls ($P < .005$); FAS < HE ($P < .005$); PFAS < HE ($P < .06$); HE < controls ($P < .10$).
* $P < .05$.
** $P < .01$.
*** $P < .001$.

during pregnancy with concentrated drinking during weekends and an average consumption per occasion of 8.9 drinks. Twelve mothers reported using marijuana, 1 used cocaine, and 3 used methaqualone ("mandrax"). A majority (70.8%) smoked, with 16.7% smoking an average of >10 cigarettes per day. On the 3D image capture, there were dose-dependent effects: for head circumference, FAS < PFAS < HE and controls; for height and weight, FAS < HE and controls; and for weight, PFAS < HE and controls. Low IQ scores seen in each group reflect poor education and socioeconomic deprivation in this community.[31,32] As expected, WISC-IV IQ scores of exposed children were lower than those of controls. The children categorized as FAS or PFAS were substantially more likely to meet clinical dysmorphology criteria than were those of the HE or control groups.

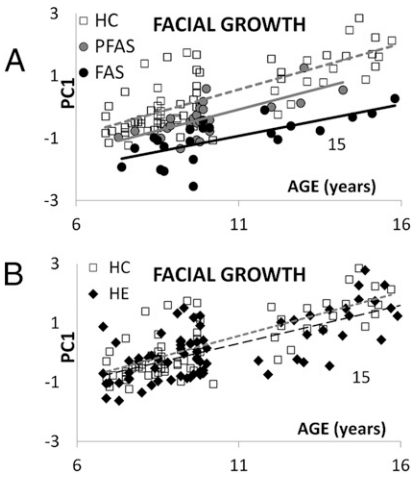

FIGURE 1
Comparison of facial growth of FASD categories. A, Facial growth indicated by PC1 for FAS and PFAS compared with HCs. B, Facial growth indicated by PC1 for HE compared with HCs. The FAS group show significantly reduced facial growth ($P < .001$) compared with healthy HCs; the PFAS group are less reduced ($P < .001$) and the HE group is marginally different ($P = .052$).

Mean Facial Growth and Dysmorphism Across the Fetal Alcohol Spectrum

In a face DSM with mixed age range, the first principal component (PC1) reflects growth. Compared with HCs, the FAS group showed significantly reduced facial growth (Fig 1A) not attributable to difference in age distribution in different categories (Table 3). The PFAS difference from HCs was less (Fig 1A) and marginal for those with HE (Fig 1B). This reduced growth caused heat maps of average FAS and PFAS faces to be almost monochromatic. Because growth retardation is discriminating in FASD, we built size and shape DSMs. When size difference overwhelms subtle shape difference, we sometimes scale average faces before comparing shape. Here, FAS, PFAS, and HE average faces were scaled using nasion-gnathion ratios, to provide shape-only comparisons (Fig 2A). Blue regions on the upper lip indicate convexity of the philtral groove, reflecting smoothness. Lower thresholds of significance for PFAS and HE groups reflect more subtle effects. In the lateral axial heat map of the average FAS face, opposing red-blue colors near inner and outer canthi confirm shortened palpebral fissures (Fig 2B). The vertical comparison reflects reduced length and upward displacement of the nose. The depth comparison identifies flat nasal bridge and glabella, malar flattening (yellow anterior zygomatic arch), and micrognathia and retrognathia (red chin). Upper lip protrusion and malar flattening

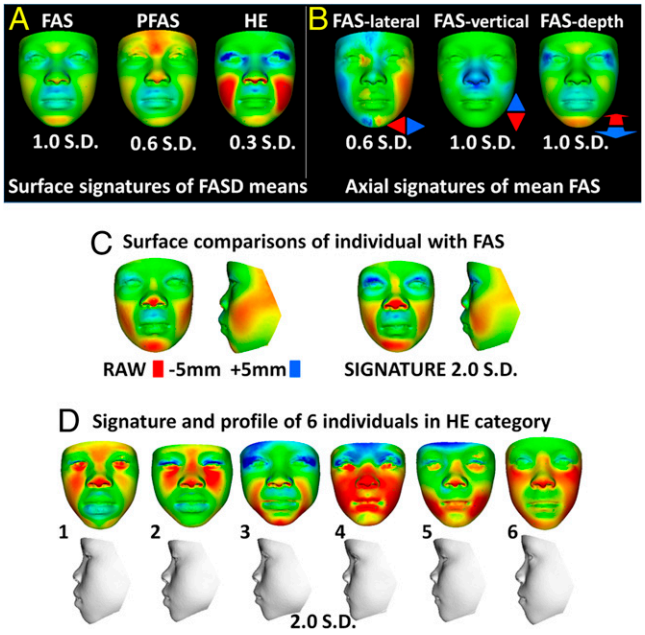

FIGURE 2

Signatures for average faces of clinical categories and for 7 individual children. A, To overcome size difference, average FAS, PFAS, and HE faces were scaled using ratio of nasion to gnathion length before normalization to give signatures reflecting shape only difference ignoring size. Red-green-blue heat maps reflect contraction-coincidence-expansion along surface normal to face at stated significance level. Terms "±1.0 SD," "±0.6 SD," and "±0.3 SD" define the upper-lower significance bounds corresponding to the extreme blue-red color range. B, Scaled axial signatures of average FAS face along 3 orthogonal axes. Opposing red-blue coloring proximal to inner and outer canthi of lateral axial signature delineates short palpebral fissures. Blue on nose of vertical axial signature reflects shortening of nose and upward displacement of nasal region. Yellow on nasal bridge and malar regions of depth or anterior-posterior axial signature highlights flattening. Blue on philtrum detects philtral smoothing. Red on chin indicates retrognathia and micrognathia. C, First heat map pair shows raw facial differences for individual with FAS from mean of 35 age-matched controls (green indicates surface coincidence; red/blue ≥5 mm contraction or expansion along surface normal). Second pair is face signature showing how raw differences of reduced face width and proptosis are reversed in relative magnitude. Philtral smoothness is indicated by blue on upper lip. Profile view reveals flat nasal bridge and malar regions, short nose, outward convexity of philtrum, and retrognathia. D, Facial dysmorphism of 6 individuals with HE highlighted by surface profiles (row 2) and heat mapped face signatures at ± 2.0 SD (row 1). More illuminating are dynamic morphs between them and age-matched control means (http://www.ucl.ac.uk/~sejjmfj/fasd_morphs.htm) revealing individuals 1 through 4 have mid-facial hypoplasia and philtral smoothing, indivuduals 1, 2, and 6 have retrognathia, and a thin upper lip is suggested in individuals 4 through 6 but not in individuals 1 through 3.

suggest rotational effects at the premaxilla. These features are clearly seen in the morph (Supplemental Movie 1).

Signature Visualizations Reveal Individual Facial Dysmorphism

Figure 2C shows portrait and profile views of a child with FAS, selected because he has classic features as well as idiosyncratic mild proptosis. The first heat map pair shows the raw difference from the mean of 35 age-matched controls, with green indicating surface coincidence and red-blue indicating ≥5 mm contraction and expansion. The second pair shows how raw differences of reduced face width and proptosis are reversed in relative magnitude after normalization. Philtral smoothness is delineated by blue on the upper lip. To reveal some features, the sensitivity of the heat map significance scale needs to be altered. Alternatively, a DSM of a more restricted area can reveal localized dysmorphism. For example, Fig 3 shows how upper lip signatures reveal where and to what degree philtral grooves are more convex and smooth. Heat maps highlighted facial dysmorphism, but the most effective visualizations were dynamic morphs between individuals and matched controls (Supplemental Movie 2). The portrait morph emphasized reduced zygomatic and gonial width, inner canthal folds, increased nose width, and philtral smoothness, especially adjacent to the columella. The profile morph highlighted flat nasal bridge and malar region, short nose, philtral groove convexity, and retrognathia.

Agreement with HC, FAS, and PFAS Categorization Based on Face Shape Alone

Closest mean (ie, relative similarity to average HC or FAS faces) induced a classification of both groups. Twenty randomly sampled 90% to 10% training-unseen test set pairs gave a mean agreement of 0.967 (Table 4) corresponding to the probability of correctly classifying a pair of faces: 1 HC and 1 FAS. Linear discriminant analysis and support vector machines were also tested, with the latter achieving perfect agreement. Classification was also completed using periorbital, perioral, perinasal, and mid-facial profile patches to determine discrimination capabilities of localized regions. The periorbit and profile patches achieved the greatest agreement. A morph between average HC and FAS profiles captured nasal bridge flattening, mid-facial hypoplasia, philtral smoothing, and retrognathia (Supplemental Movie 3). As expected, the addition of PFAS individuals depressed agreement with clinical categorization because of increased heterogeneity due to relaxing growth and head size criteria (see Table 1). Although face-based classification for HC versus FAS plus PFAS was inferior to that of HC versus FAS, the face profile performed consistently well at 0.91 to 0.93 (Table 4). This concurs with mid-line neurofacial effects found in murine models of ethanol exposure.[43,44] Inclusion and exclusion of siblings did not affect classification.

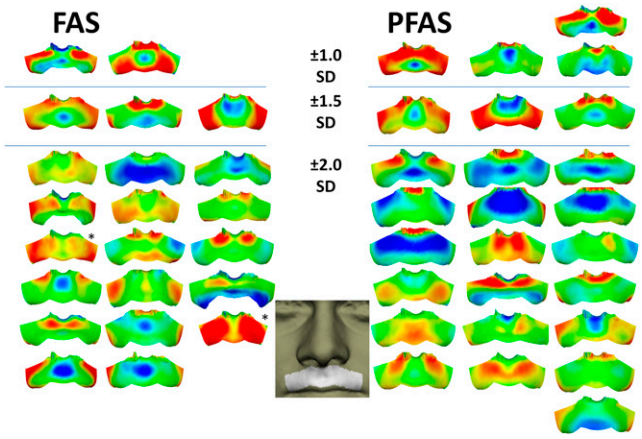

FIGURE 3
Examples of upper lip signatures. Convex philtral grooves are typically delineated by blue regions surrounded by green. When the upper lip is much reduced in size compared with matched controls, convexity may be highlighted as a yellow or green region surrounded by red*. Insert shows region of upper lip modeled.

Face Signature Graphs Provide a Panorama of Facial Dysmorphism Across the Fetal Alcohol Spectrum

Figure 4 shows face signatures of 107 alcohol-exposed individuals normalized against HCs: FAS (rows 1 and 2), PFAS (rows 3 and 4), and HE (rows 5–9). As the focus moves from FAS to PFAS to HE, predominant hues change from red-green to green-blue, reflecting greater facial growth and shape difference. Sixteen individuals were omitted due to insufficient controls for normalization. The corresponding signature graph is shown in Fig 5A. Individual signatures offer a panorama of facial dysmorphism across the fetal alcohol spectrum. Graph connectivity links individuals with similar facial dysmorphism (see Fig 5A insets or higher magnification in Supplemental Fig 2). Typically, peripheral (resp. central) nodes represent individuals with strong (resp. mild) dysmorphism. Figure 5B is a color-labeled form coding clinical categories: FAS (red), PFAS (blue), and HE (green). Signatures between the upper right of Fig 5A and cluster 8 are almost all labeled HE. Their mainly green-blue hue emphasizes coincidence or expansion compared with controls. In contrast, signatures from the lower left of the graph toward cluster 15 are largely FAS and PFAS (mostly red-green, reflecting contraction or coincidence compared with controls).

TABLE 4 Agreement of Face and Face Patch Classification With Clinical Categorization

	HC Versus FAS			HC Versus FAS + PFAS		
	CM	LDA	SVM	CM	LDA	SVM
Face	0.967	0.967	1.00	0.892	0.909	0.909
Periorbit	0.983	0.917	0.967	0.892	0.900	0.892
Perioral	0.850	0.850	0.884	0.883	0.883	0.883
Perinasal	0.833	0.850	0.934	0.825	0.825	0.817
Profile	0.933	0.933	0.917	0.925	0.933	0.917

Each classification rate was estimated as the mean area under ROC curves of 20 cross-validation trials and corresponds to the probability of correctly classifying 2 individuals, 1 taken from each of the 2 groups being compared. Closest mean classification labels members of 2 groups by the name of the group whose mean is most similar. For linear discriminant analysis (LDA), the goal is a linear combination of principal component modes that exhibits the largest difference in the subgroup means relative to the within-group variance. Support vector machines, or large margin classifiers, focus on individual cases in the overlap of the subgroups to be classified that help to define a separating surface with largest margin between the subgroups. In addition to the full face, patches of the face were also considered in isolation: periorbit, perioral, perinasal, and profile. CM, closest mean; SVM, support vector machines.

Subset of the HE Group Has Facial Dysmorphism That Is More FAS-like Than HC-like

The second color coding of the signature graph (Fig 5C) shows all FAS and PFAS nodes as red, whereas HE nodes are green circles or squares. Squares highlight 28 HE signatures below cluster 8 with greater FAS or PFAS affinity. This was preserved even when controls were introduced to form a new signature graph (Supplemental Fig 3A). Closer scrutiny of these individuals detected more FAS-like facial features. For example, 6 individuals (Fig 2D) display a flat mid-face and/or flat nasal bridge, as shown by their profile (row 2) and red-yellow regions in heat maps (row 1). In dynamic morphs between them and matched control means (http://www.ucl.ac.uk/~sejjmfj/fasd_morphs.htm), individuals 1 through 4 showed mid-facial hypoplasia and philtral smoothing; individuals 1, 2, and 6 have retrognathia; and a thin upper lip is suggested in individuals 4 through 6 but not in individuals 1 through 3.

We normalized the HE group against themselves to produce another signature graph (Supplemental Fig 3B) with largely red-green and green-blue face signatures at opposite ends. In the color-coded form (Supplemental Fig 3C), the previously "squared" signatures form a homogeneous aggregate. Thus, they have been selected objectively in 2 signature graphs: first, by FAS/PFAS affinity after normalization against HCs and, second, as a homogeneous subgraph after normalization against HE.

Neurobehavioral Differences in the HE Group Reflect Presence or Absence of FAS-like Facial Features

No differences were found for prenatal alcohol exposure, maternal age, parity, or smoking between the HE subgroup with FAS/PFAS affinity (nonsyndromal heavy exposed with FAS/PFAS-like face signature [HE1]) versus the HE subgroup

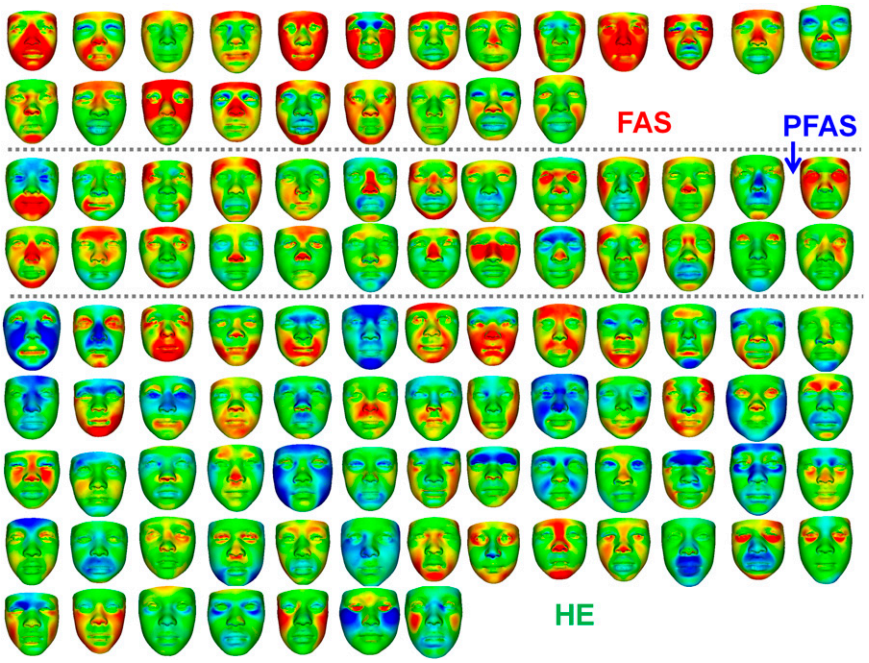

FIGURE 4

Face signatures of 107 alcohol-exposed individuals, Face signatures at ±2.0 SD of 107 alcohol-exposed individuals with normalization against 35 age-matched healthy controls: FAS (rows 1 and 2), PFAS (rows 3 and 4), and HE (rows 5–9). The term "±2.0 SD" defines the upper-lower significance bounds corresponding to the extreme blue-red color range.

with control affinity (nonsyndromal heavy exposed with more control-like face signature [HE2]) ($P > .10$). However, HE1 was markedly more affected on neurocognitive measures than HE2, especially for WISC IV Verbal Comprehension IQ and CVLT-C (Table 5). Mean HE1 performance was comparable to FAS, whereas HE2 resembled controls.

DISCUSSION

As with genetic syndromes, facial gestalt recognition is a clue to FAS diagnosis. Milder FASD phenotypes and overlapping features in syndromes make recognition challenging. Computer-based facial analysis shows potential for recognizing FAS facial characteristics, but without an accurate test for FASD, studies inducing classification schemes only assess agreement with clinical categorization, which is not standardized. Therefore, comparison of such studies should consider subjects, facial features, and pattern-matching adopted as well as accuracy of agreement.

In a study of a different sample of South African children of mixed ancestry (17 with FAS and 17 controls), clinical categorization considered facial gestalt, growth and head circumference, IQ, behavior and prenatal alcohol exposure.[10] Each face was represented by a set of 3D landmarks and image-based classification used discriminant function analysis. Agreement with clinical categorization involved drop-one-out-testing to produce sensitivity-specificity pairs of 100%:91% at 5 years and 76%:83% at 12 years, suggesting FAS facial dysmorphism becomes less distinct with age.

For a subset of our cohort (36 with FAS and 31 controls) and a Finnish (50 with FAS and 32 controls) cohort,[9] clinical categorization was identical to ours. The 3D face laser scans underwent feature extraction before classification using neural networks. Evaluation involved a 66%:33% training-unseen test set pair for each cohort and their combination. The sensitivity-specificity results (88.2%:100% for Finnish cohort; 91.7%:90% for South African children of mixed ancestry; 82.75%:76.2% for their combination) and selection of different features for each cohort suggest a varying effect depending on ethnicity.

The study pioneering face evaluation[13] for the 4-digit code[14] involved 84 controls. Clinical categorization of FAS for 42 individuals was facial gestalt recognition from 2-dimensional photographs. Each face was characterized by ratio of palpebral fissure length to inner canthal separation and measures of philtrum smoothness and upper lip thinness. Classification involved stepwise discriminant function analysis. The evaluation used one randomly generated 50%:50% training-unseen test set pair, and agreement was calculated at one value of the induced discriminant function. Rather than calculating area under an ROC curve, this selects a single point on it. Discriminant functions were derived for combinations of assessing philtrum smoothness and upper lip thinness by use of a subjective Likert scale or

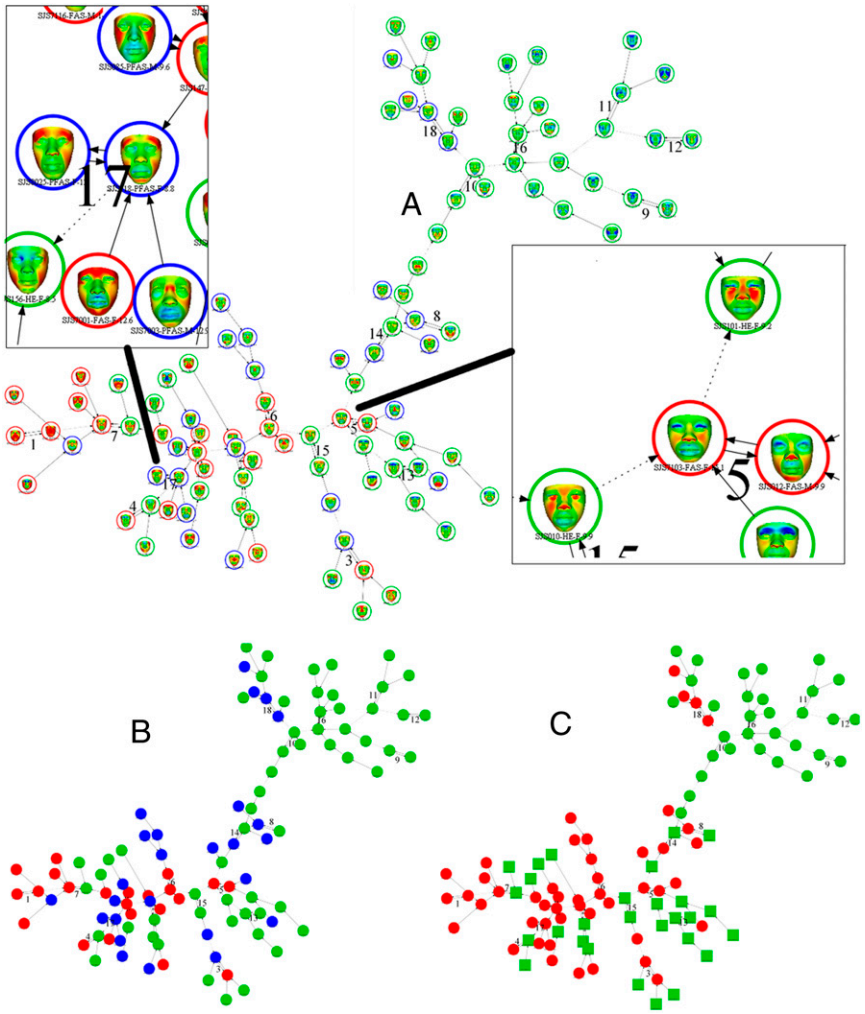

FIGURE 5

Face signature graphs of 107 alcohol-exposed individuals. A, Face signature graph of 18 clusters arising from normalization against controls of 107 children with clinical categorization of FAS, PFAS, or HE. Magnified insets show links between individuals with similar face signatures. B, Color-coded form of signature graph in A. Red/blue/green–filled nodes represent FAS/PFAS/HE individuals, respectively. C, Alternative form of B where FAS and PFAS nodes are red and HE nodes are green. HE individuals in close proximity to FAS/PFAS aggregation are depicted by squares, not circles.

objective measures of philtrum luminosity and upper lip circularity. Classification using the Likert scales generated sensitivity-specificity of 100%:100% on the unseen test data at a single value of the discriminant function. Similar results were quoted for discriminant functions derived from all 126 subjects that necessarily involved no unseen testing. This study included individuals from different ethnic backgrounds and controls with different genetic conditions.

Our primary aim was to identify strategies for recognizing facial dysmorphism across the fetal alcohol spectrum. Our ultimate goal is to help pediatricians identify children at high risk for deficits due to prenatal alcohol exposure from different ethnic backgrounds and across wide age ranges. We used pattern matching algorithms and ROC-based analysis of multiple random training-unseen test set pairs to estimate agreement of face classification with a multifaceted diagnostic phenotype (Table 1). Our results showed that DSM-based representation of 3D face shape alone achieved perfect agreement for FAS and good agreement for FAS plus PFAS. Mid-facial profile performed consistently well for both FAS and FAS plus PFAS and will be investigated further in future studies.

We demonstrated that heat map comparisons and dynamic morphing of faces to matched controls revealed facial dysmorphism that was otherwise overlooked. Finally, ignoring clinical categorization, we built graphs linking individuals with similar face signatures. The signature graph using controls for normalization of 107 exposed individuals provided a panorama of facial dysmorphism across the fetal alcohol spectrum. The FAS/PFAS individuals clustered, almost entirely, at

TABLE 5 Verbal IQ and Learning by FASD Classification

	FAS	PFAS	HE1	HE2	HC	*t* HE1 Versus HE2
WISC-IV IQ[a]						
Verbal Comprehension Index	65.4 (13.4)	63.0 (8.0)	65.5 (12.9)	73.3 (10.4)	73.3 (12.3)	−1.80*
CVLT-C[b]						
List A total correct	42.7 (12.0)	41.5 (11.4)	40.0 (11.1)	47.3 (9.0)	45.8 (9.5)	−2.02**
Recognition discrimination	88.5 (11.4)	88.3 (12.3)	84.3 (20.1)	93.7 (6.0)	93.2 (9.4)	−1.89*

Values are mean (SD). Standard scores are presented for the WISC-IV; mean number of correct responses is presented for the CVLT-C. HE1, nonsyndromal heavy exposed with FAS/PFAS-like face signature; HE2, nonsyndromal heavy exposed with more control-like face signature.

[a] n = 9 FAS, 19 PFAS, 13 HE1, 16 HE2, 22 HC.

[b] n = 13 FAS, 19 PFAS, 13 HE1, 18 HE2, 38 HC.

* $P < .08$.

** $P < .05$.

one end of the graph, with 28 individuals with HE, whereas the remaining individuals with HE clustered at the opposite end. In addition, when individuals with HE were normalized against themselves, the signature graph isolated the same 28 individuals with HE. This HE subgroup showed few of the classic FAS facial features, but flat nasal bridge, malar flattening, philtral smoothing, and micrognathia and retrognathia were revealed in dynamic morphs between the individuals and matched control means.

Different approaches have been advanced for delineating a behavioral profile for alcohol-related neurodevelopmental disorder,[44,45] but a definitive profile has not yet been identified. It is noteworthy that facial dysmorphism detected in individuals with HE showing closer affinity with the FAS/PFAS aggregation proved to be indicative of neurocognitive deficits approaching 0.5 SD, compared with controls and other children with HE. Signature graph nodes could be color filled at intensities reflecting BMI or by colors reflecting neurobehavior status to investigate links between facial dysmorphism and other biomarkers.

In summary, this study identified novel strategies for detecting facial effects of prenatal alcohol exposure. Heat maps of faces and dynamic morphs to matched controls substantially enhanced the unaided appreciation of facial form. More substantial testing is planned in South Africa, the United States, and the Ukraine. The Collaborative Initiative on Fetal Alcohol Spectrum Disorders plans to make our face visualization tools available to participating dysmorphologists in the coming year. After evaluation and modification, they will be distributed more widely. The 3D cameras are now used routinely by surgeons and orthodontists. Increasingly, there are mobile device apps and websites offering conversion from 2 dimensions to 3 dimensions.[47] Stereo webcams[48] are appearing in laptops for face recognition for security and communication. Thus, 3D face photography is becoming more widely available with the potential to support 3D face shape analysis.

ACKNOWLEDGMENTS

We thank Sr Maggie September, who organized and helped coordinate the clinics and has made major contributions to the maintenance of the University of Cape Town longitudinal cohorts since their inception; to the UCT and Wayne State University research staffs for their help in data collection and analysis; and to Neil Dodge and Catherine O'Leary, who analyzed the WISC IV-IQ and CVLT-C data. We thank Denis Viljoen, Anna Susan Marais, and Julie Croxford for their contributions to the recruitment of the Cape Town prospective longitudinal cohort. We are also grateful to the mothers and children in the Cape Town cohort for their long-term participation in the study.

REFERENCES

1. Jones KL, Robinson LK, Bakhireva LN, et al. Accuracy of the diagnosis of physical features of fetal alcohol syndrome by paediatricians after specialized training. *Pediatrics*. 2006;118:1734–1738
2. Hoyme HE, May PA, Kalberg WO, et al. A practical clinical approach to diagnosis of fetal alcohol spectrum disorders: clarification of the 1996 institute of medicine criteria. *Pediatrics*. 2005;115(1):39–47
3. Jones KL, Smith DW. Recognition of the fetal alcohol syndrome in early infancy. *Lancet*. 1973;302(7836):999–1001
4. CDC. Fetal alcohol syndrome: guidelines for referral and diagnosis. (2004) www.cdc.gov/ncbddd/fasd/documents/fas_guidelines_accessible.pdf
5. Moore ES, Ward RE, Jamison PL, Morris CA, Bader PI, Hall BD. The subtle facial signs of prenatal exposure to alcohol: an anthropometric approach. *J Pediatr*. 2001;139(2):215–219
6. Moore ES, Ward RE, Jamison PL, Morris CA, Bader PI, Hall BD. New perspectives on the face in fetal alcohol syndrome: what anthropometry tells us. *Am J Med Genet*. 2002;109(4):249–260
7. Moore ES, Ward RE, Wetherill LF, et al; CIFASD. Unique facial features distinguish fetal alcohol syndrome patients and controls in diverse ethnic populations. *Alcohol Clin Exp Res*. 2007;31(10):1707–1713
8. Mutsvangwa T, Douglas TS. Morphometric analysis of facial landmark data to characterize the facial phenotype associated with fetal alcohol syndrome. *J Anat*. 2007;210(2):209–220
9. Fang S, McLaughlin J, Fang J, et al; Collaborative Initiative on Fetal Alcohol Spectrum Disorders. Automated diagnosis of fetal alcohol syndrome using 3D facial image analysis. *Orthod Craniofac Res*. 2008;11(3):162–171
10. Mutsvangwa TE, Meintjes EM, Viljoen DL, Douglas TS. Morphometric analysis and classification of the facial phenotype associated with fetal alcohol syndrome in 5- and 12-year-old children. *Am J Med Genet A*. 2010;152A(1):32–41
11. Douglas TS, Mutsvangwa TE. A review of facial image analysis for delineation of the facial phenotype associated with fetal alcohol syndrome. *Am J Med Genet A*. 2010;152A(2):528–536
12. Foroud T, Wetherill L, Vinci-Booher S, et al. Relation over time between facial measurements and cognitive outcomes in fetal alcohol-exposed children. *Alcohol Clin Exp Res*. 2012;36(9):1634–1646
13. Astley SJ, Clarren SK. A case definition and photographic screening tool for the facial phenotype of fetal alcohol syndrome. *J Pediatr*. 1996;129(1):33–41
14. Astley SJ, Clarren SK. Diagnosing the full spectrum of fetal alcohol-exposed individuals: introducing the 4-digit diagnostic code. *Alcohol Alcohol*. 2000;35(4):400–410
15. Klingenberg CP, Wetherill L, Rogers J, et al; CIFASD Consortium. Prenatal alcohol exposure alters the patterns of facial asymmetry. *Alcohol*. 2010;44(7-8):649–657
16. Bhuiyan ZA, Klein M, Hammond P, et al. Genotype-phenotype correlations of 39 patients with Cornelia De Lange syndrome: the Dutch experience. *J Med Genet*. 2006;43(7):568–575
17. Cox-Brinkman J, Vedder A, Hollak C, et al. Three-dimensional face shape in Fabry disease. *Eur J Hum Genet*. 2007;15(5):535–542

18. Hammond P, Hutton TJ, Allanson JE, et al. 3D analysis of facial morphology. *Am J Med Genet A*. 2004;126A(4):339–348
19. Hammond P, Hutton TJ, Allanson JE, et al. Discriminating power of localized three-dimensional facial morphology. *Am J Hum Genet*. 2005;77(6):999–1010
20. Hammond P. The use of 3D face shape modelling in dysmorphology. *Arch Dis Child*. 2007;92(12):1120–1126
21. Hammond P, Forster-Gibson C, Chudley AE, et al. Face-brain asymmetry in autism spectrum disorders. *Mol Psychiatry*. 2008;13(6):614–623
22. Hammond P, Hannes F, Suttie M, et al. Fine grained facial phenotype-genotype analysis in Wolf-Hirschhorn syndrome. *Eur J Hum Genet*. 2012;20(1):33–40
23. Hutton TJ, Buxton BF, Hammond P, Potts HW. Estimating average growth trajectories in shape-space using kernel smoothing. *IEEE Trans Med Imaging*. 2003;22(6):747–753
24. Kasperavičiūtė D, Catarino CB, Chinthapalli K, et al. Uncovering genomic causes of co-morbidity in epilepsy: gene-driven phenotypic characterization of rare microdeletions. *PLoS ONE*. 2011;6(8):e23182
25. Tassabehji M, Hammond P, Karmiloff-Smith A, et al. GTF2IRD1 in craniofacial development of humans and mice. *Science*. 2005;310(5751):1184–1187
26. Tobin JL, DiFranco M, Eichers E, et al. Defects of Shh transduction and neural crest cell migration underlie craniofacial dysmorphology in Bardet-Biedl syndrome. *Proc Natl Acad Sci USA*. 2008;105(18):6714–6719
27. Lipinski RJ, Hammond P, O'Leary-Moore SK, et al. Stage-specific ethanol exposure causes unique face-brain dysmorphology patterns in a mouse model of fetal alcohol spectrum disorder. *PLoS ONE*. 2012;7(8):e43067 doi:10.1371/journal.pone.0043067
28. Sturn A, Quackenbush J, Trajanoski Z. Genesis: cluster analysis of microarray data. Bioinformatics. 2002;18 (1):207–208
29. Hammond P, Suttie M, Hennekam RC, Allanson J, Shore EM, Kaplan FS. The face signature of fibrodysplasia ossificans progressiva. *Am J Med Genet A*. 2012;158A(6):1368–1380
30. Hammond P, Suttie MJ. Large-scale objective phenotyping of 3D facial morphology. *Hum Mutat*. 2012;33(5):817–825
31. Jacobson SW, Stanton ME, Molteno CD, et al. Impaired eyeblink conditioning in children with fetal alcohol syndrome. *Alcohol Clin Exp Res*. 2008;32(2):365–372
32. Jacobson SW, Stanton ME, Dodge NC, et al. Impaired delay and trace eyeblink conditioning in school-age children with fetal alcohol syndrome. *Alcohol Clin Exp Res*. 2011;35(2):250–264
33. Jacobson SW, Chiodo LM, Jacobson JL, Sokol RJ. Validity of maternal report of alcohol, cocaine, and smoking during pregnancy in relation to infant neurobehavioral outcome. *Pediatrics*. 2002;109:815–825
34. Meintjes EM, Jacobson JL, Molteno CD, et al. An FMRI study of number processing in children with fetal alcohol syndrome. *Alcohol Clin Exp Res*. 2010;34(8):1450–1464
35. Astley SJ, Clarren SK. Measuring the facial phenotype of individuals with prenatal alcohol exposure: correlations with brain dysfunction. *Alcohol Alcohol*. 2001;36(2):147–159
36. Carter RC, Jacobson JL, Molteno CD, et al. Effects of heavy prenatal alcohol exposure and iron deficiency anemia on child growth and body composition through age 9 years. *Alcohol Clin Exp Res*. 2012;36(11):1973–82
37. Wechsler D. *Wechsler Intelligence Scale for Children–4th Edition (WISC-IV)*. San Antonio, TX: Harcourt Assessment; 2003
38. Delis DC, Kramer JH, Kaplan E, Ober BA. *California Verbal Learning Test–Children's Version*. New York, NY: The Psychological Corporation; 1994
39. Mattson SN, Roebuck TM. Acquisition and retention of verbal and nonverbal information in children with heavy prenatal alcohol exposure. *Alcohol Clin Exp Res*. 2002;26(6):875–882
40. O'Leary CE, Thomas KGF, Molteno CD, Jacobson JL, Jacobson SW. Verbal learning and memory in fetal alcohol spectrum disorder: findings from Cape Town and Detroit. *Alcohol Clin Exp Res*. 2011;35(s1):111A
41. Gwilliam JR, Cunningham SJ, Hutton TJ. Reproducibility of soft tissue landmarks on three-dimensional facial scans. *Eur J Orthod*. 2006;28(5):408–415
42. Ellson J, Gansber E, Koutsofios L, North S, Woodhull G. *Lecture Notes in Computer Science*, vol. 2265: *Graphviz- Open Source Graph Drawing Tools*. Berlin Heidelberg, Germany: Springer-Verlag Berlin Heidelberg; 2002:594–597
43. Roussotte FF, Sulik KK, Mattson SN, et al. Regional brain volume reductions relate to facial dysmorphology and neurocognitive function in fetal alcohol spectrum disorders. *Hum Brain Mapp*. 2012;33(4):920–937
44. Mattson SN, Crocker N, Nguyen TT. Fetal alcohol spectrum disorders: neuropsychological and behavioral features. *Neuropsychol Rev*. 2011;21(2):81–101
45. Jacobson SW, Jacobson JL, Stanton ME, Meintjes EM, Molteno CD. Biobehavioral markers of adverse effect in fetal alcohol spectrum disorders. *Neuropsychol Rev*. 2011;21(2):148–166
46. Thomas IT, Gaitantzis YA, Frias JL. Palpebral fissure length from 29 weeks gestation to 14 years. *J Pediatr*. 1987;111(2):267–268
47. Autodesk, Inc www.123dapp.com
48. Minoru 3D webcam, www.minoru3d.com

(Continued from first page)

www.pediatrics.org/cgi/doi/10.1542/peds.2012-1371

doi:10.1542/peds.2012-1371

Accepted for publication Nov 19, 2012

Address correspondence to Prof Peter Hammond, Molecular Medicine Unit, UCL Institute of Child Health, 30 Guilford St, London WC1N 1EH, UK.
E-mail: p.hammond@ucl.ac.uk

PEDIATRICS (ISSN Numbers: Print, 0031-4005; Online, 1098-4275).

FINANCIAL DISCLOSURE: *The authors have indicated they have no financial relationships relevant to this article to disclose.*

FUNDING: This international collaborative study is supported by grants from the National Institute on Alcohol Abuse and Alcoholism (NIAAA): U01AA014809 (Dr Foroud); U01AA014790, U24AA014815, U24AA014828, U24AA014830, and R01AA016781 (Dr Jacobson); an administrative supplement to R01AA09524 (Dr Jacobson); and U24AA014811 (Dr Riley). Additional funds were provided by the National Institutes of Health Office of Research on Minority Health (Dr Jacobson) and the Joseph Young Sr Fund from the state of Michigan (Dr Jacobson). This work was conducted in conjunction with the Collaborative Initiative on Fetal Alcohol Spectrum Disorders (CIFASD), which is funded by grants from the NIAAA. Additional information about CIFASD can be found at www.cifasd.org. Funded by the National Institutes of Health (NIH).

Facial Dysmorphism Across the Fetal Alcohol Spectrum

Michael Suttie, Tatiana Foroud, Leah Wetherill, Joseph L. Jacobson, Christopher D. Molteno, Ernesta M. Meintjes, H. Eugene Hoyme, Nathaniel Khaole, Luther K. Robinson, Edward P. Riley, Sandra W. Jacobson and Peter Hammond

Pediatrics 2013;131;e779; originally published online February 25, 2013;
DOI: 10.1542/peds.2012-1371

PEDIATRICS®
OFFICIAL JOURNAL OF THE AMERICAN ACADEMY OF PEDIATRICS

Facial Dysmorphism Across the Fetal Alcohol Spectrum

Michael Suttie, Tatiana Foroud, Leah Wetherill, Joseph L. Jacobson, Christopher D. Molteno, Ernesta M. Meintjes, H. Eugene Hoyme, Nathaniel Khaole, Luther K. Robinson, Edward P. Riley, Sandra W. Jacobson and Peter Hammond

Pediatrics 2013;131;e779; originally published online February 25, 2013;
DOI: 10.1542/peds.2012-1371